Draft version May 9, 2016
Preprint typeset using LaTeX style emulateapj v. 01/23/15

CONSTRAINING DARK MATTER NEUTRINO EMISSION USING REALISTIC SOLAR MODELS

J. Lopes
CENTRA, Physics Department, Instituto Superior Técnico, Universidade de Lisboa, Portugal
Draft version May 9, 2016

ABSTRACT

Hypothetical Dark Matter (DM) weakly interacting massive particles (WIMP) populating the Milky Way halo can be gravitationally captured by the Sun. There, WIMPs will annihilate, creating a neutrino flux which detection would shed light on the nature of DM. The idea of using the neutrino flux arriving from the Sun to constrain DM models is not new. However, current analysis tend to overlook the astrophysical implications on the computation of such constraints. Moreover, WIMPs captured in the Sun will provide additional energy transport and production mechanisms which can have impact in the Solar structure.In this work we used a robust and consistent stellar evolution code to constrain DM models, exploiting the limits on the neutrino flux arriving from the Sun measured by the Super-Kamiokande and IceCube detectors.

We found that WIMPs in the Sun will cool the Solar core and increase its central density, which, in extreme scenarios, can lead to Solar models in stark disagreement with observations. These effects, however, are negligible for the parameter space favoured by theoretical considerations on the DM production in standard cosmology. Based on this conclusion, we obtained the upper limits on the WIMP scattering cross-section, for two different WIMP annihilation scenarios: the widely used model with constant annihilation cross-section, and the commonly overlooked model of thermally annihilating DM. These limits are sensible to the current uncertainty on Solar models, showing a maximum variation of 25 %, depending on the WIMP annihilation channel.

1. INTRODUCTION

The joint effort of physicists in the last four decades has resulted in solid evidence, not only at astrophysical but also cosmological scales, which leave no doubt that our Universe is mainly populated by a still undetected non-interactive type of matter, the so-called Dark Matter (DM), which nature is still unknown. Amongst the numerous theories devised to solve this problem, the picture of a Weakly Interactive Massive Particle (WIMP) arises as the most favourable, since the DM abundance inferred today from the Cosmic Microwave Background (CMB) matches the abundance of a relic particle with an annihilation cross-section of the order of the weak scale. Furthermore, new particle physics theories motivated by different reasons, provide natural candidates for this type of matter, making this a highly interdisciplinary field of investigation.

In the picture of particle DM, WIMPs that populate the Milky Way can be gravitationally captured by the Sun (Steigman et al. 1978). Since WIMPs are mandatorily stable, they will accumulate inside Sun, and annihilate to Standard Model (SM) particles, which will produce a distinctive neutrino signal which can be detected in current and projected neutrino detectors, providing an excellent indirect survey to DM properties, that has been extensively studied (Silk et al. 1985) (Gaisser et al. 1986) (Griest & Seckel 1987) (Wilkström & Edsjö 2009).

However, most indirect DM searches focus on simple models where WIMPs are Majorana particles and annihilate through an *s*-wave, velocity independent, thermally averaged cross-section, $\langle \sigma v \rangle$. In these models, it usual to fix $\langle \sigma v \rangle \sim 10^{-26}$ cm^{3}s^{-1} , in order to respect the DM density (Kolb & Turner 1989), which is precisely determined from CMB measurements (Ade et al. 2015). Theoretically, the DM abundance, is defined by the moment of WIMP *freeze out*, which happens when the Universe's temperature drops below the WIMPs mass, resulting in the decoupling of DM particles from the primordial Universe thermal bath. This will result in a constant number of WIMPs per comoving volume which will leave a footprint in the abundance measured today.

Despite the fact that the usual approach in literature is to use a constant thermally averaged cross-section, there are a large number of well-motivated models which have a p-wave contribution, (i.e. a dependence in the relative velocity between WIMPs) to the annihilation cross-section which can be dominant. Models where DM is a Majorana particle, such as the *neutralino*, a natural candidate which arises from the *Minimal Supersymmetric* extension to the Standard model (MSSM), s-wave annihilation to fermion anti-fermion pairs is helicity suppressed by a factor of $(m_f/m_\chi)^2$, where m_χ is the WIMPs mass (Sheldon et al. 2010) (Goldberg 1983). Furthermore, due to CP conservation, final states with CP=+1, are only accessible through p-wave annihilations (s-wave states for two identical Majorana fermions are CP=-1). Hence, neutralino annihilation to HH or any combination of the vectorial bosons W and Z, can only occur trough p-wave annihilation (Drees & Nojiri 1992). Another well known example, is the case of Parity conserving minimal extensions to the SM with a fermionic DM candidate - a gauge singlet Dirac fermion - in which annihilation to scalar states with even parity, such as $\chi\chi \rightarrow HH$, doesn't receive contribution from the s-wave annihilations (Kim and Lee 2007).

In this work we obtained limits on the DM-nucleon scattering cross-section placed by neutrino telescopes, for two different WIMP models: the standard scenario where annihilation occurs through the s-wave channel; the commonly overlooked model where p-wave annihilation is the leading contribution to the total annihilation cross-section. Formally, each of these models consists in accounting for the first and second terms, respectively, in the thermally averaged annihilation cross-section expansion,

$$\langle \sigma v \rangle = a + b \left\langle v^2 \right\rangle + \mathcal{O}(\langle v^4 \rangle) \simeq a + b' x^{-1}, \qquad (1)$$

where $x = m_\chi / T$, and where we also assumed that higher order terms with $\mathcal{O}\left(\langle v^4 \rangle\right)$, are negligible. The coefficients a and b in 1 are assumed constant and obtained taking into account the DM density at the time of freeze-out, which is roughly the same as today (see sec. 4.1).

We used a modified stellar evolution code to simulate the evolution of the Sun within a DM halo, taking into account the treatment of the interplay between the Sun and DM. Since WIMPs captured inside the Sun can contribute as additional energy transport and production mechanisms, we also investigated the parameter space for which the impact of DM can produce sizeable departures from the current understanding of the Sun, the so-called Standard Solar Model (SSM).

We start by briefly describing the stellar evolution code in section 2 where we also test the SSM (Solar model without DM) produced with the code against Helioseismic and Solar neutrino observations. In sec. 3 we describe the formalism used to treat the interplay between DM and the Sun, and we study the impacts the former can have on the latter's structure. In sec. 4 we obtain the limits on the DM-nucleon cross-section, for the s and p-wave scenarios, placed by the Super-Kamiokande (SK) and IceCube (IC) experiments. We end with some conclusions and final remarks in sec. 5.

2. THE SOLAR MODEL

Our stellar evolution code is based on CESAM (Morel 1997) and has been further developed to include not only the DM capture and annihilation formalism, but also the framework for energy transport and distribution inside the Sun (Lopes et al. 2011) (see sec. 3).

CESAM is an open-source group of routines which consistently computes a one dimensional quasi hydrostatic stellar evolution. The code is originally written within a modular structure, i.e., giving the user the possibility to use different formalisms for the physical processes taking part in the Sun.

2.1. *Reference Standard Solar Model*

We started this work by choosing the physical inputs given to the stellar evolution code in order to obtain a realistic baseline reference model (RM) without the effects of DM. This is a mandatory step if one hopes to use the Sun as a laboratory to investigate the DM nature. The standard Solar inputs chosen for the RM are thus used in all the subsequent simulations.

The physical input chosen for the RM is thoroughly described in the main document. The decision regarding the set of heavy element abundances however deserves a brief commentary. The chemical composition of such elements in the Sun has been estimated by different authors. The most recent determination by Asplund et al. (2009) (hereafter AGSS09) results in Solar models in disagreement with Helioseismological and Solar neutrino observations. Surprisingly, this problem, known as the *Solar Abundance Problem* (see for e.g. Serenelli (2010)), is somewhat alleviated if the older estimation by Grevesse et al. (1998) (hereafter GS98) is used instead. Despite the fact that the most recent abundances were determined with highly complex and consistent models, there is no consensus on which of the mixtures describes best the actual Sun. For this reason we decided to adopt the AGSS09 abundances as the reference mixture, although repeating the computations for the GS98 abundances in order to study the impact that this uncertainty has on our results.

The RM is evolved from the Zero Age Main Sequence (ZAMS) until its present age, $t_\odot = 4.6 \times 10^9$ Gyr, according to the fundamental equations of stellar structure. An ansatz is assigned to the initial helium abundance Y and mixing length parameter $\alpha_{\rm MLT}$ (a parameter which describes the convective energy transport in the Sun). The final model output is then compared with well known solar observables and the free parameters Y and $\alpha_{\rm MLT}$ are accordingly adjusted before the evolution is redone with those updated values. This process is repeated until a precision of 10^{-5} on the Solar radius, luminosity, and metallicity at the surface is achieved. By doing this, we assure that the RM is calibrated to achieve a SSM (Turck-Chieze & Lopes 1993) in full agreement with the predominant Solar models used in the literature (Bahcall et al. 2005) (Serenelli et al. 2009).

In fig. 1 we plotted the difference between the modelled and observed Sound Speed Profile (SSP) for the RM models and for BS05, one of the most used SSM in the literature (Bahcall et al. 2005). The RM shows a remarkable agreement with the Helioseismic data, with a maximum deviation of 1.3 % located beneath the bottom of the convective zone at $r \simeq 0.7 R_\odot$. As expected, the model evolved with the older GS98 abundances yields variations in the SSP lower than RM(AGSS09) by at least a factor of 2, with a maximum difference of 0.5%. It is also worth noticing that our reference model is consistent with the Solar model by BS05.

The Solar neutrinos produced in the thermonuclear reactions taking part within the Sun also pose an excellent test to the SSM. In particular, the flux of neutrinos produced in the ^{8}B and ^{7}Be reactions of the pp nuclear chain reaction, have production regions of $\Phi_{^8\rm B} \simeq 0.04 R_\odot$ and $\Phi_{^7\rm Be} \simeq 0.06 R_\odot$ (Lopes et al. 2010) respectively, thus constituting an extraordinary probe to the inner regions of the Solar core.

In table 1 we show the ^{8}B and ^{7}Be neutrino fluxes obtained in the reference model evolved with the AGSS09 and GS98 abundances, as well as the fluxes for the model BS05. For comparative reasons, we also show the fluxes measured by neutrino ground based telescopes. While the fluxes obtained with the GS98 model are in agreement with the values measured by the Borexino experiment, the reference model shows a deficit of $\sim 13\%$ and $\sim 30\%$ (21%) on the ^{8}B and ^{7}Be Borexino (SNO) fluxes

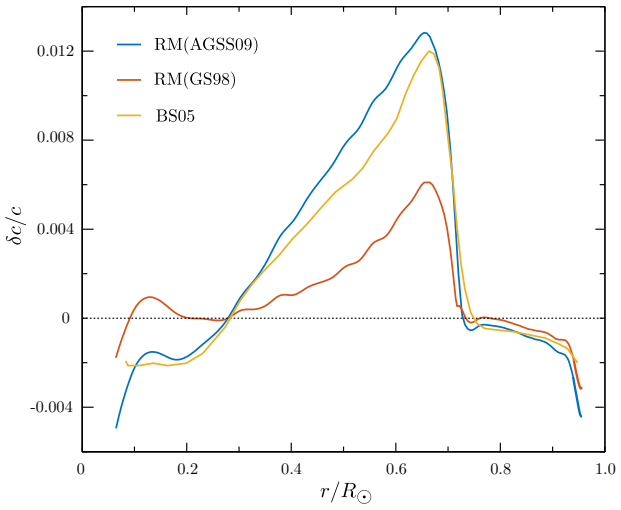

FIG. 1.— Comparison between experimental and modelled SSP inside the Sun. The experimental data is interpolated from Basu et al. (2009). Three curves are shown: the SSP for RM(AGSS09); the SSP for RM(GS98); the SSP for the most widely used SSM in the literature (Bahcall et al. 2005) (using a previous abundance mixture by Asplund et al. (2005), hereafter AGS05).

TABLE 1
MODELLED AND EXPERIMENTAL SOLAR NEUTRINO FLUXES ORIGINATED IN THE ^{7}Be AND ^{8}B THERMONUCLEAR REACTIONS.

	Modelled Solar Neutrino fluxes [a]	
	^{7}Be	^{8}B
RM(AGSS09)	4.22	4.14
RM(GS98)	4.98	5.89
BS05(AGS05)	4.38	4.59
	Experimental Solar Neutrino fluxes	
Refs	^{7}Be	^{8}B
SNO (2013) [b]	-	$5.25 \pm 0.16^{+0.19}_{-0.20}$
Borexino (2010) [c]	-	5.88 ± 0.65
Borexino (2011) [d]	4.87 ± 0.24	-

[a]The ^{7}Be and ^{8}B fluxes are in units of [10^9 cm^{-2} s^{-1}] and [10^6cm^{-2} s^{-1}] respectively
[b]Aharmim et al. (2013)
[c]Bellini et al. (2010)
[d]Bellini et al. (2011)

respectively. Since the thermonuclear reactions, hence, the Solar neutrino fluxes, increase with the temperature, this suggests that our reference model has a core somewhat cooler than the actual Sun.

3. DARK MATTER AND THE SUN

WIMPs in the Solar vicinity can be gravitationally capture by the Sun. There, they will act as additional energy production and transport mechanisms. The efficiency of these processes will depend on the DM properties, and on the number of WIMPs accumulated in the Sun, which is defined by the capture and annihilation processes.

3.1. *Number of WIMPs in the Sun*

The number of WIMPs in the Sun is governed by three distinct processes: capture, annihilation and evaporation (which is the inverse reaction of capture). When the evaporation process is negligible, which is our case since we are studying WIMPs with $m_\chi > 4$ GeV (Busoni et al. 2013), the number of WIMPs is given by

$$\frac{\mathrm{d}N_\chi}{\mathrm{d}t} = C_\odot - A_\odot N_\chi^2, \tag{2}$$

where $C_\odot$ is the capture rate, and

$$A_\odot \equiv \int_\odot \langle\sigma v\rangle n_\chi(r)^2 \mathrm{d}r^3, \tag{3}$$

is the annihilation coefficient, which is integrated over the Sun's volume taking into account the WIMPs normalized distribution, $n_\chi(r)$. The capture rate, $C_\odot$, which accounts for capture by the different i elements present in the Sun, is given by (Gould 1987)

$$C_\odot = \sum_i \int_0^{R_\odot} 4\pi r^2 \int_0^\infty \frac{f(u)}{u} w \Omega^-_{v_\mathrm{e}(r),i}(w,r)\mathrm{d}u\mathrm{d}r. \tag{4}$$

The kinetic factor $\Omega^-_{v_\mathrm{e}(r),i}(w,r)$, which measures the rate of scattering of a WIMP from an initial velocity w to a final velocity lower than the local escape velocity $v_\mathrm{e}(r)$, is directly proportional to the density of nucleons in the solar plasma, and the DM-nucleon scattering cross-section. As a first approximation, it is usual to assume that DM couples with barionic matter through Spin Dependent (SD) (only important for interactions with Hydrogen) and Spin Independent (SI) effective scattering cross-sections.

Equation 2 has a straightforward solution, which yields

$$N_\chi(t) = \sqrt{\frac{C_\odot}{A_\odot}} \tanh(\sqrt{C_\odot A_\odot} t). \tag{5}$$

Defining the equilibrium time-scale $t_\mathrm{eq} \equiv \left(C_\odot A_\odot\right)^{-\frac{1}{2}}$, which represents the time needed to achieve equilibrium between WIMP capture and annihilation, the number of WIMPs in the Sun today is in equilibrium if $t_\mathrm{eq} \ll t_\odot$, where $t_\odot = 4.6$ Gyr. In that case, equation 5 simplifies to

$$N_\chi(t_\odot) \simeq \sqrt{\frac{C_\odot}{A_\odot}}, \tag{6}$$

and the annihilation rate is simply given by

$$\Gamma_A = \frac{1}{2} N_\chi^2 A_\odot \simeq \frac{1}{2} C_\odot. \tag{7}$$

As we can see by equation 7, if the WIMP number equilibrium has been attained, the annihilation rate, Γ_A, and consequently the neutrino flux, will depend exclusively on the capture rate, which means that no conclusions can be made regarding the nature of the DM annihilation cross-section using data from neutrino experiments.

3.2. *Energy production and transport*

The transport of energy by WIMPs within the Solar structure is governed by the Knudsen number (Faulkner et al. 1986),

$$K(t) = \frac{l(0,t)}{r_\chi(t)}, \tag{8}$$

which is the ratio between the WIMPs mean free path in the center of the Sun, and the length-scale of its distribution (Spergel & Press 1985),

$$r_\chi(t) = \left(\frac{9}{4\pi} \frac{kT_c(t)}{G\rho_c(t)m_\chi} \right)^{\frac{1}{2}}, \quad (9)$$

where $T_c(t)$ and $\rho_c(t)$ are the Solar central temperature and density respectively. If $K \ll 1$, wimps are in Local Thermodynamic Equilibrium (LTE) with the Solar plasma and reflect its temperature, i.e. $T_\chi(r) = T_\odot(r)$ (Gould & Raffelt 1990). If $K \gtrsim 1$, WIMPs will transport energy non-locally and will have an isothermal distribution characterized by a unique temperature, T_χ (Spergel & Press 1985). To compute the WIMP distribution and energy transport contribution for arbitrary $K(t)$, it is usual to interpolate between the LTE and isothermal scenarios. The interpolation is a computed using a suppression factor, function of $K(t)$, which accounts for the departure of the LTE regime.

The pair annihilation of WIMPs can also impact the structure of the Sun, providing an additional source of energy. The energy contribution from WIMPs at each height of the star is given by (Yoon et al. 2008)

$$\epsilon_\chi(r) = \frac{2}{3} \frac{m_\chi n_\chi^2(r)}{\rho_{\odot(r)}} \langle \sigma v \rangle, \quad (10)$$

where the factor 3/2 accounts for the energy carried by the neutrinos produced DM annihilation, which energy loss in the Solar plasma is approximately negligible.

3.3. *Impact*

The original stellar evolution code was modified by (Lopes et al. 2011) to include the DM phenomena in the computation of the stellar evolution. At each age step of evolution the code obtains the number of WIMPs in the Sun by computing the capture and annihilation rates. The energy production and transport contributions to the stellar structure equations are then computed, and the equations are adjusted accordingly. In order to study the impact of WIMPs in the Sun, we carried out a large number of models with arbitrary scattering and annihilation cross-sections [1]. We found that the energy production and transport of WIMPs in the Sun will lead to a lower central temperature and higher central density of barionic nuclei in the Solar plasma. As expected, these effects are mainly felt in the Solar core, since that is the region where WIMPs cluster. However, in order to obtain a non-negligible effect, WIMPs need to be somewhat light, $m_\chi = 10$ GeV, have a relatively large scattering cross-section, $\sigma_{SI} \simeq 10^{-38}$ cm^2 and $\sigma_{SD} \simeq 10^{-36}$cm^2, with small annihilation cross-sections, $\langle \sigma v \rangle \simeq 10^{-31}$ cm^3 s^{-1}.

In fig. 2 we plotted the difference in the SSP between the RM and models evolved with different WIMP parameters. In order to study the maximal impact of WIMPs in the Sun, we chose the benchmark value of $m_\chi = 5$ GeV, which is the minimum mass for which we can assure that evaporation is negligible (Busoni et al. 2013). Despite some of the models exhibiting a considerable variation in the SSP for $r \lesssim 0.1 R_\odot$, almost nothing can be inferred about the validity of such models due to the high experimental and theoretical uncertainty on the measured sound speed in the Solar core (see fig. 1).

Solar neutrinos on the other hand, are highly sensitive to variations in the Solar central temperature, and thus can strongly constrain this quantity (Bahcall & Ulrich (1988) have shown that the Boron neutrino flux has a dependence of $\Phi_{^8B} \propto T_c^{18}$).

In fig. 3 we show the variation in the ^{8}B Solar neutrino flux for models evolved with different WIMP models with respect to the RM(AGSS09). The strong dependence on the temperature will cause important variations in the fluxes of Solar neutrinos, which in the extreme cases exhibits a variation of 50% and 40% for the SD and SI scattering cross-sections, respectively. Using the values in 1 we can estimate both the theoretical and experimental uncertainty on the ^{8}B Solar neutrino flux to be $\simeq 30\%$ and $\simeq 5\%$, respectively. This conservative estimation allows to confidently rule out DM models producing a variation in the ^{8}B neutrino flux larger than 35% (white solid line in fig. 3).

Although we found a region of the WIMP parameter space for which the impact in the Solar model will cause a considerable departure from the SSM, it consists of parameters that are either hardly constrained from direct and indirect detection experiments or are in contradiction with theoretical predictions for currently measured DM abundance. Nonetheless, the analysis carried out in this section provides helpful insight on the region of DM parameters for which the processes of WIMP energy transport and production cannot be negligible.

4. NEUTRINOS FROM ANNIHILATING DARK MATTER

WIMPs captured inside the Sun can annihilate, creating SM particles from which only neutrinos will escape the Solar plasma without loosing considerable energy. In this section we obtain the limits on the DM-nucleon SI and SD scattering cross-section placed by the SK and IC detectors. Differently from sec 3, here we will focus on WIMP models which annihilation cross-section is in compliance with the standard picture of thermally produced DM in the early ages of the Universe.

4.1. *Dark Matter production in the early Universe*

The DM particle comoving number density n_χ is governed the Boltzmann equation (Kolb & Turner 1989)

$$\frac{\mathrm{d}n_\chi}{\mathrm{d}t} = -3Hn_\chi - \langle \sigma v \rangle (n_\chi^2 - n_{\chi,\mathrm{eq}}^2), \quad (11)$$

where H is the Hubble parameter, and $n_{\chi,\mathrm{eq}}$ is the WIMP's number density when in equilibrium with the thermal plasma. Equation 11 takes into account the Universe's expansion rate as well as the annihilation and production of WIMPs from the thermal plasma (first and second terms in the r.h.s. of eq. 11). To simplify equation 11 it is usual to use the law of entropy conservation defining the number density n_{eq} in terms of the universe's total entropy $Y \equiv n_\chi/s$, and changing the independent variable from t to $x \equiv m_\chi/T$, where T is the photon temperature.

[1] In fact, the concept of WIMP doesnt allow for arbitrary large or small annihilation cross-sections (see sec. 4.1). Nonetheless, in this stage our interest is mainly the impact of general models of particle DM in the Sun, and for that reason we use models with arbitrarily small annihilation cross-sections

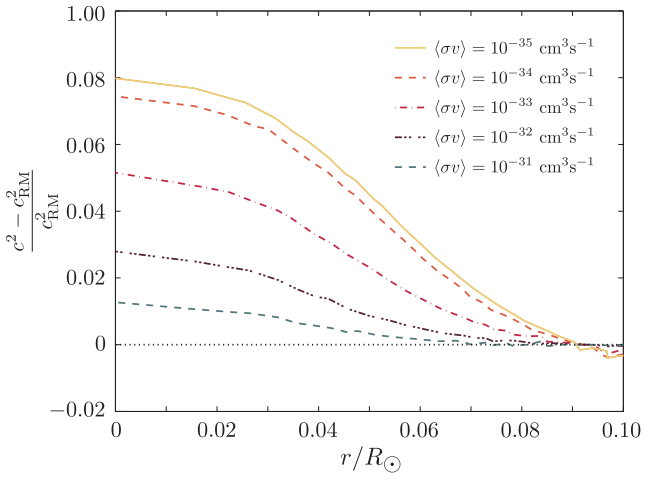

(a) Spin Independent ($\sigma_{\rm SI} = 10^{37}$cm^2).

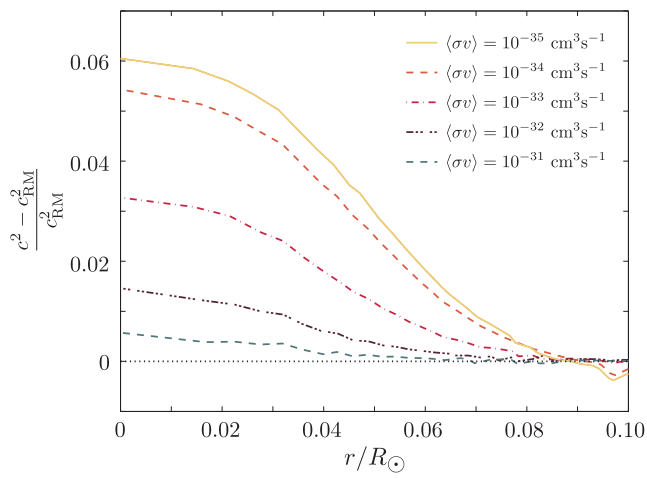

(b) Spin Dependent ($\sigma_{\rm SD} = 3 \times 10^{36}$cm^2)

FIG. 2.— Squared sound-speed difference between RM(AGSS09) and models evolved with DM with different annihilation cross-section (see legend). The WIMPs have a mass of $m_\chi = 5$ GeV and a galactic halo density $\rho_\chi = 0.38$GeV cm^3.

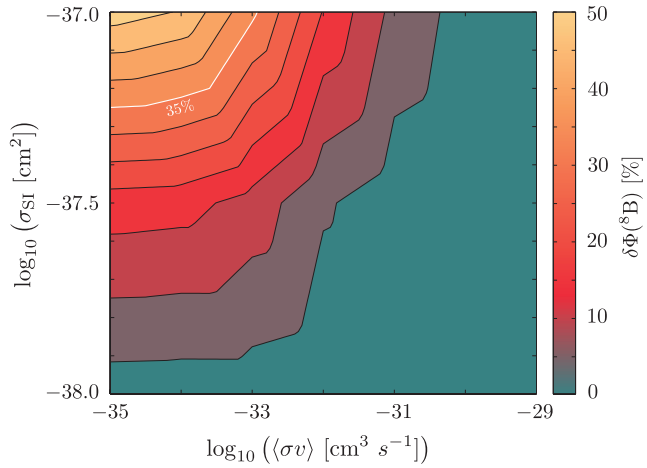

(a) ^{8}B Flux variation for $\sigma_{\rm SI}$.

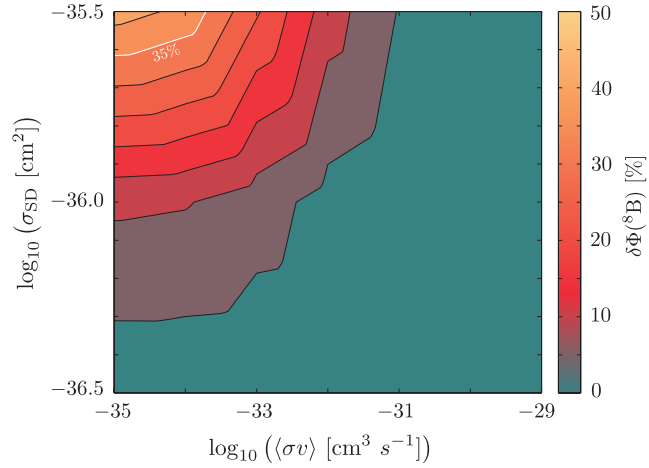

(b) ^{8}B Flux variation for $\sigma_{\rm SD}$

FIG. 3.— Impact of DM particles in the Boron Solar neutrino flux. The difference is computed with respect to the RM(AGSS09). This figure was obtained from models evolved within a DM halo of WIMPS with $m_\chi = 5$ GeV with an halo density $\rho_\chi = 0.38$ GeV cm^3.

For the standard s-wave case (first term in the r.h.s. of eq. 1), eq. 11 can be solved analytically for the limits $x \ll x_{\rm F}$ and $x \gg x_{\rm F}$, where $x_{\rm F}$ is the moment when WIMPs decouple from the primordial thermal bath. This computation has been carried out by different authors (Kolb & Turner 1989) (Gondolo & Gelmini 1991), who have shown that in order to obtain an abundance coherent with observations of the CMB, WIMPS are required to have $\langle\sigma v\rangle \simeq 3 \times 10^{-26}$ cm^3 s^{-1}.

For the p-wave case however, eq.11 needs to be numerically solved. Focusing on the second term in the r.h.s. of 1 ($a \ll b'$), the Boltzmann equation eq. 11 can be written as

$$\frac{dY}{dx} = -\Lambda x^{-3}(Y^2 - Y_{\rm eq}^2), \tag{12}$$

with

$$\Lambda = \sqrt{\frac{\pi}{45 g_\rho}} g_s m_{Pl} m_\chi b', \tag{13}$$

where m_{Pl} is the planck's mass. The effective number of relativistic degrees of freedom in the Universe contributing to the energy density, g_ρ, can be approximated by a step-function (Dent et al. 2010) and in the epoch of WIMP freeze-out is essentially the same as the effective number of relativistic degrees of freedom contributing to the total entropy, g_s. For this reason, hereafter we will use $g \equiv g_s \equiv g_\rho$.

In the early Universe (for low x), Y tracks the equilibrium number density $Y_{\rm eq}$ since WIMPs are constantly annihilating and being produced. When the annihilation rate drops below the expansion rate, WIMPs freeze-out, i.e. they fall out of thermodynamic equilibrium and their abundance is fixed. Assuming that WIMPs usually freeze-out at temperatures below their mass $T_F \ll m_\chi$ (Jungman et al. 1996), we can use a non-relativistic Maxwell-Boltzmann distribution for $Y_{\rm eq}$ for a WIMP with g_χ degrees of freedom,

$$Y_{\rm eq}(x) = \frac{45}{2\pi^4}\sqrt{\frac{\pi}{8}}\frac{g_\chi}{g}x^{3/2}e^{-x}. \quad (14)$$

Numerically solving equation 12 with 13 and 14, using the condition that $Y = Y_{\rm eq}$ at $x = 1$ we obtained the WIMP number density today, Y_0 (fig. 4). Finally, we

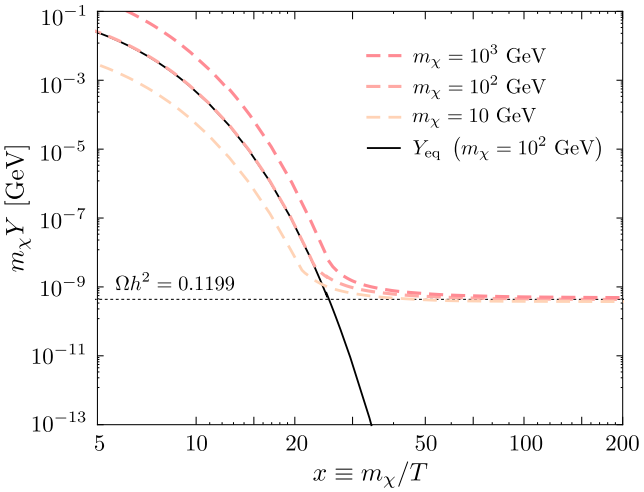

FIG. 4.— WIMP number density evolution for different m_χ solved numerically. Solid line: Equilibrium abundance (for the sake of simplicity it is only shown the equilibrium abundance for $m_\chi = 100$ GeV); Dashed: WIMP number density for different m_χ; Dotted: Number density corresponding to the WIMP relic density (eq. 15) measured from the CMB today for different m_χ.

computed the WIMP relic density using

$$\Omega_\chi h^2 \equiv \frac{\rho_\chi}{\rho_{\rm critical}} = 2,74\times10^8 m_\chi Y_0, \quad (15)$$

from where we obtained the value b' which best reproduces the relic abundance measured from the CMB, $\Omega_\chi h^2 = 0,1199$ (Ade et al. 2015) for a WIMP of $m_\chi = 100$ GeV is $b' = 9,60\times10^{-25}$ cm^{3}s^{-1}. It is important to stress that this result is mainly independent from the mass, as we can see in fig. 4, except for logarithmic corrections. We can also see by fig. 4 that WIMPs freeze-out at a temperature of roughly $x_F \gtrsim 20$ which is consistent with the hypothesis that freeze-out occurs when WIMPs are non-relativistic.

4.2. *The Isothermal Limit*

To study how WIMPs are distributed in the Solar medium, we computed the Knudsen Number (eq. 8) at the present age, $K(t_\odot)$, in the WIMP parameter region of interest (fig. 5).

Due to the low scattering cross-sections, WIMPs will orbit the Sun several times before scattering with a barionic nuclei, which means that in this region, K is always larger than 1. This allows us to assume that WIMPs will always be isothermally distributed, following a Boltzmann distribution of characteristic temperature T_χ (Gould & Raffelt 1990),

$$n_\chi(r) \simeq n_{\chi,{\rm iso}}(r) = \frac{e^{-m_\chi\phi(r)/kT_\chi}}{\int_\odot e^{-m_\chi\phi(r')/kT_\chi}{\rm d}r'^3}, \quad (16)$$

where $\phi(r)$ is the gravitational potential inside the Sun. Taking into account that WIMPs tend to strongly cluster on the Solar core (for example, $r_\chi \simeq 0.05R_\odot$ for $m_\chi = 4$ GeV and $r_\chi < 0.01R_\odot$ for $m_\chi \gtrsim 150$ GeV) it is to accurate approximate the potential $\phi(r)$ for $r < r_\chi$ by assuming a constant Solar central density $\rho_{\rm c}$, which yields $\phi(r) \propto \rho_{\rm c} r^2$, resulting in a much simpler expression for the WIMP distribution,

$$n_\chi(r) \simeq \frac{e^{-\frac{r^2}{r_\chi^2}}}{\pi^{\frac{3}{2}} r_\chi^3}. \quad (17)$$

In equation 17 we also used eq. 9 assuming that $T_\chi \simeq T_{\rm C}$, which is accurate for higher m_χ. For lower masses, $m_\chi \approx 5$ GeV, the error in this approximation is always lower than 7% regarding the temperature, which is somewhat mitigated by the fact that WIMPs with lower masses will be close to equilibrium (see sec. 4.3).

4.3. *Annihilation Rate and Equilibrium Regime*

In the usual approach, where WIMPs annihilate through s-wave, the number of WIMPs in the Sun is in the equilibrium in all the parameter region of interest, and the last equality of eq. 7 is an excellent approximation. In this case, the annihilate rate can be trivially computed and does not depend explicitly on the annihilation coefficient. However, in the p-wave case, the annihilation coefficient is given by,

$$A_\odot = \frac{b'}{m_\chi}T_\chi\int n_\chi(r)^2{\rm d}r^3, \quad (18)$$

which will generally yield $t_{\rm eq} \gtrsim t_\odot$, rendering the approximation in eq. 7 invalid. For example, WIMPs with $m_\chi \gtrsim 5$ GeV will mainly populate the inner 10 % of the Solar radius, where the temperature is approximately 1.5×10^7 K, which is at least 4 orders of magnitude lower than the freeze-out temperature for a WIMP with the same characteristics. This means that $\langle\sigma v\rangle$ for WIMPs annihilating in the Sun will be dramatically lower than $\langle\sigma v\rangle$ at freeze-out, which will in turn increase the equilibrium time-scale.

Eq. 18 can be simplified taking into account the isothermal approximation in eq. 17, which yields,

$$A_\odot = \frac{T_{\rm c}}{m_\chi}\frac{b'}{4\pi r_\chi^3}\left[\sqrt{\frac{2}{\pi}}{\rm Erf}\left(\sqrt{2}\frac{R_\odot}{r_\chi}\right) - \frac{4}{\pi}\frac{R_\odot}{r_\chi}e^{-2\frac{R_\odot^2}{r_\chi^2}}\right] \quad (19)$$

where $R_\odot \simeq 6.96\times10^{10}$ cm is the Solar radius. Taking into account that in our case $R_\odot \gg r_\chi$, we can simplify eq. 19 to the final annihilation coefficient expression,

$$A_\odot \simeq \frac{T_{\rm C}}{m_\chi}\frac{b'}{\sqrt{8}\pi^{\frac{3}{2}}r_\chi^3}, \quad (20)$$

which is independent of the Sun radius, as expected.

In figure 6 we computed the annihilation rate for WIMPs isothermally distributed (eq. 17) in the s and p-wave scenarios for different WIMP masses and scattering cross-sections. As we can see, for larger scattering cross sections ($\sigma_{SD} = 10^{-36}$ cm^2 and $\sigma_{SI} = 10^{-39}$ cm^2) there is almost no difference between the two cases, since

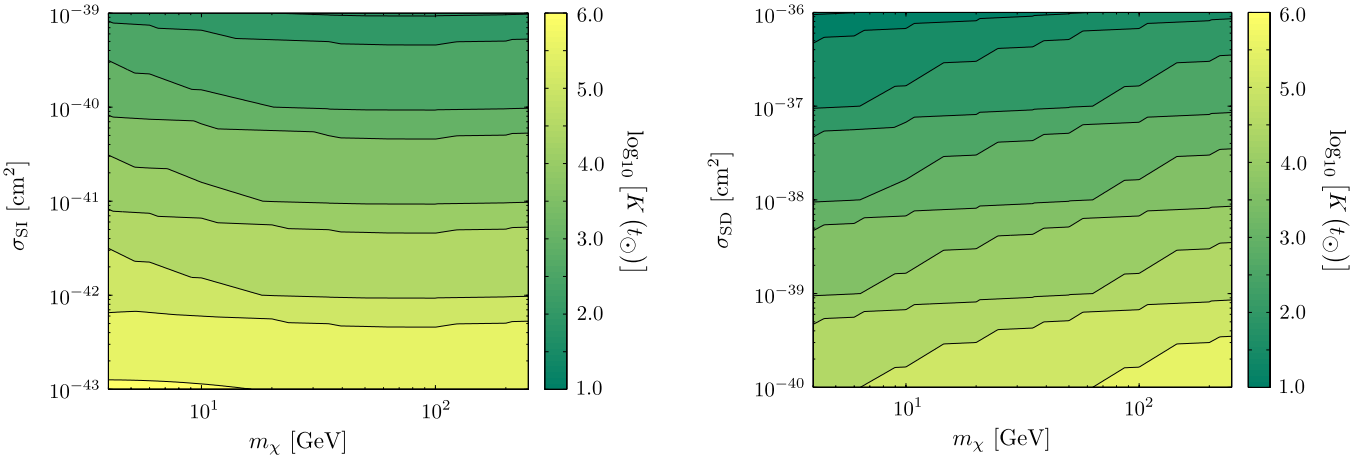

(a) Spin Independent (b) Spin Dependent

FIG. 5.— The Knudsen number (8) in the WIMP parameter region of interest. Colour scale is logarithmic.

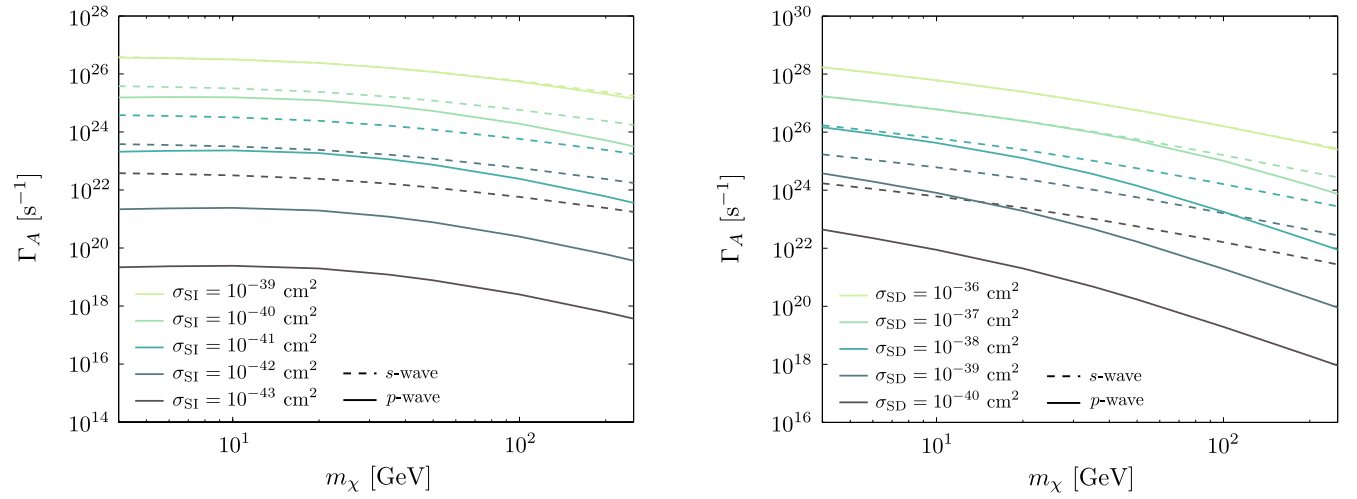

(a) Spin Independent (b) Spin Dependent

FIG. 6.— Annihilation Rate for different SD and SI cross-sections. Dashed: Annihilation rate for models with s-wave annihilation. Solid: Annihilation rate for models with p-wave annihilation.

the number of WIMPs has achieved equilibrium in the two cases. However, as we increase the mass and decrease the scattering cross-section, there is a large difference between the s and p-wave scenarios. This is also visible in figure 7, where we plotted the hyperbolic tangent in eq. 2 for the p-wave case,

$$K \equiv \tanh\left(t_\odot/t_{\rm eq}\right), \tag{21}$$

which measures the departure from WIMP number equilibrium. Regions where the number of WIMPs is far from equilibrium, i.e. where $K \ll 1$, the annihilation rate (fig. 6) will be lower in the p-wave case. In fact, for smaller scattering cross-sections ($\sigma_{SD} = 10^{-40}$ cm^2 and $\sigma_{SI} = 10^{-43}$ cm^2) and higher masses, the difference between the two annihilation cases can be of several orders of magnitude, which will result in more relaxed constraints, as we will show in the next section.

4.4. *Limits from neutrino telescopes*

The neutrino flux from WIMP annihilation in the Sun is given by

$$\Phi_\nu = \frac{\Gamma_A}{4\pi r^2} \sum_i {\rm BR}_i \int \frac{{\rm d}N_\nu}{{\rm d}E_\nu} {\rm d}E_\nu, \tag{22}$$

where the sum is done over the i possible annihilation channels, with branching ratio ${\rm BR}_i$ and spectra ${\rm d}N_\nu/{\rm d}E_\nu$. Note that the branching ratios for each annihilation channel are not known for a general WIMP model. However, most WIMPs annihilate predominantly to one particular state, such as $b\bar{b}$, $\tau^+\tau^-$ and W^+W^-. The neutrino signal can be detected on Earth using large Čerenkov detectors, such as the ICECUBE, in the South Pole, and the SUPER-KAMIOKANDE, in the *Kamioka Mine*, Japan. To compute the neutrino flux measured here on Earth, we used WIMPSIM (Blennow et al. 2008) (integrated with our stellar evolution code), which

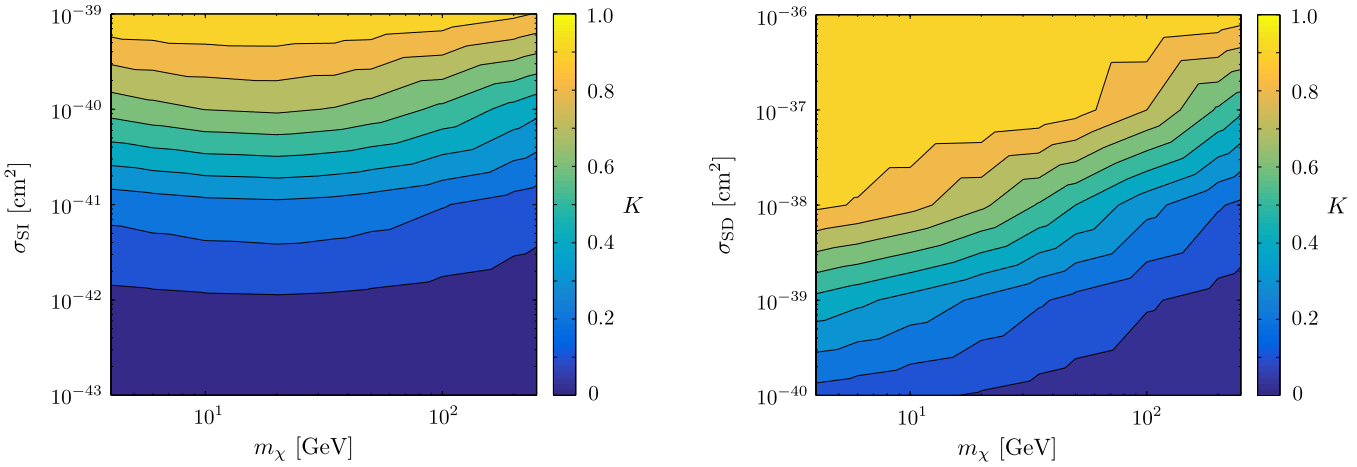

(a) Spin Independent

(b) Spin Dependent

FIG. 7.— Equilibrium parameter for the actual Sun, $K(t_\odot)$, for the WIMP parameter region of interest in the p-wave scenario. Yellow regions are in equilibrium and the annihilation rate is independent of the annihilation cross-section. Blue regions are not in equilibrium and the annihilation rate depends on the annihilation cross-section.

uses an event-based framework. WIMPSIM computes WIMP annihilation to SM particles, and their subsequent hadronization or decay to neutrinos using PYTHIA 6.400 (Sjöstrand et al. 2006). After that, it propagates the neutrino signal through the Solar medium and vacuum, using a three-flavour oscillation framework and taking into account neutrino charged currents (CC) and neutral currents (NC) with the Solar nuclei, which will have impact in the neutrino spectra for higher energies.

The upper-limits on the neutrino flux from WIMP annihilation in the IC and SK were converted to annihilation rates using WIMPSIM. The annihilation rates, Γ_A, where converted into upper limits on the scattering cross-section (SD and SI) using our stellar evolution code to compute DM capture and annihilation. In fig. 8 we plotted the upper limits for s and p-wave annihilation, as well as regions of interest from different direct detection experiments (see figure caption for references).

As expected, for regions where $t_{eq} \ll t_\odot$, the limits on the scattering cross-section for WIMP models with dominant p-wave annihilation are coincident with the limits for the standard s-wave case. However, as we increase m_χ and decrease the scattering cross-section, the number of WIMPs will fall out of equilibrium resulting in smaller annihilation rates, as shown in sec. 4.3, which will convert to upper limits on the SD and SI scattering cross-sections above the standard case, specially for higher masses.

The result obtained also shows that as experiments are built to further constrain the neutrino signal from WIMP annihilation, it will be continuously harder to survey lower scattering cross-sections for models with dominant p-wave annihilation, since we will enter the parameter region where the number of WIMPs is far from equilibrium (see fig. 7). In this limit, where $t_{eq} \gg t_\odot$, the number of WIMPs in the Sun can be approximated by

$$N_\chi(t_\odot) = \sqrt{\frac{C_\odot}{A_\odot}}\,\tanh(\sqrt{C_\odot A_\odot}\,t_\odot) \simeq C_\odot t_\odot, \qquad (23)$$

resulting in

$$\Gamma_A \simeq \frac{1}{2}\left(C_\odot t_\odot\right)^2 A_\odot, \qquad \left(C_\odot \propto \sigma_{\rm SD/SI}\right), \qquad (24)$$

which means that if we are able to lower the upper limit in the neutrino flux by a factor of 10, it will result in lowering the upper limit on the scattering cross-section by a factor of approximately 3, for models with dominant p-wave annihilation.

In order to study how the current uncertainty on the overall Solar models affect our results, we repeated the process described above using the GS98 heavy element abundances, with a higher metallicity to Hydrogen ratio ($(Z/X)_\odot = 0.0178$ for AGSS09 and $(Z/X)_\odot = 0.0229$ for GS98). We found that the largest source of uncertainty to the limits shown in fig. 8 is the capture rate $C_\odot$, which for SD scattering is larger for AGSS09 ($\sim 4\%$ independent of m_χ), and for SI scattering is larger ($\sim 14\%$ for $m_\chi = 10$ GeV and $\sim 20\%$ for $m_\chi = 200$ GeV) for GS98. This difference, which is a direct consequence of the difference in $(Z/X)_\odot$ between models, can have impact in the upper limits for $\sigma_{\rm SD/SI}$ since the annihilation rate Γ_A depends on the number of WIMPs N_χ, which in turn depends on $C_\odot$. The difference in the central temperature between Solar models evolved with the mixture by GS98 and AGSS09, ($\sim 2\%$ higher T_c for GS98) will produce an uncertainty in the annihilation coefficient (eq. 20) which is sob dominant compared to the uncertainty in the capture rate. In the overall picture, for Solar models with GS98, upper limits on the SD cross-section will be $\sim 4\%$ more relaxed, while upper limits in the SI cross-section will be stronger ($\sim 10\%$ for lower m_χ and reaching 25 % for $m_\chi \simeq 100$ GeV).

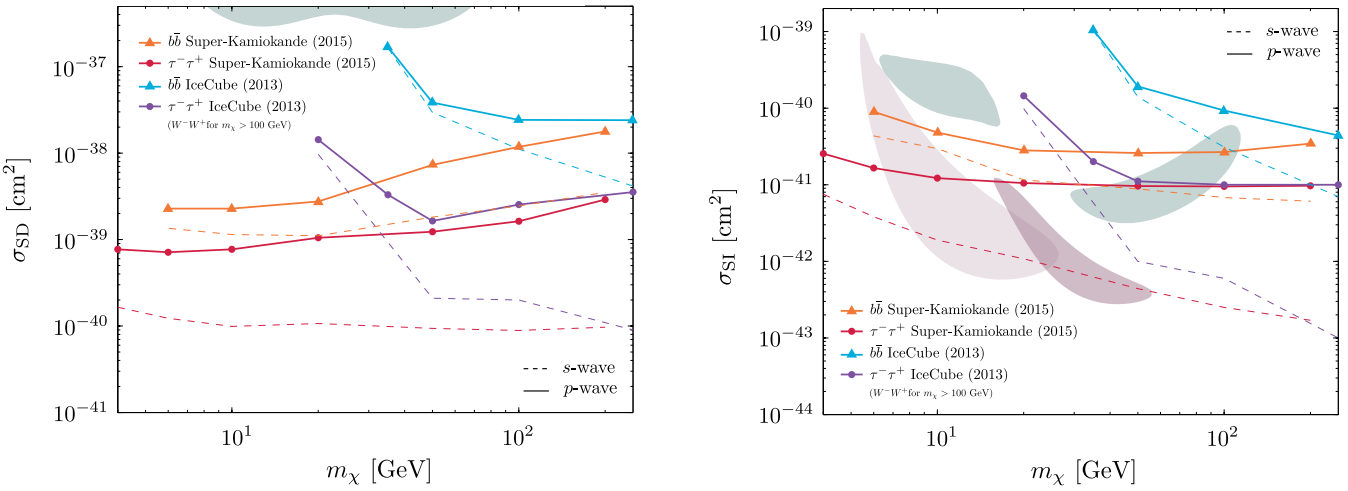

(a) Spin dependent (b) Spin independent

FIG. 8.— Limits in the SD and SI scattering cross-section placed by neutrino the SK and IC detectors. Dashed: Limits for the standard s-wave annihilation case. Solid: Limits for p-wave annihilation. Also shown are the results from different direct detection experiments. Pink shaded: CDMS II Si at 95 % C.L. (Agnese et al. 2013); Purple shaded: DAMA/LIBRA at 3σ C.L. (Bernabei et al. 2008); Purple shaded: CRESSTII at 2σ C.L. (Angloher et al. 2012).

5. CONCLUSIONS

Dark Matter particles trapped in the Sun will annihilate and create a neutrino signal which can be used to survey its properties. In this article we studied the neutrino emission for two simple models corresponding to the scenarios in which the main contribution for the annihilation comes for the s and p-wave channel, respectively.

We started by studying the impact of DM particles in the structure of the Sun. We found that Solar models evolved within an halo of light WIMPs ($m_\chi \simeq 5$ GeV) with large scattering cross-sections and small annihilation cross-sections will have a lower central temperature and higher central density, when compared to the SSM. In the extreme scenarios, Solar models will have Solar neutrino fluxes dramatically different from those computed from the SSM, with variations that can reach 50% for the ^{8}B Solar neutrino flux. Taking into account theoretical and experimental uncertainties on the computation of this flux, we are able to confidently rule-out the WIMP parameter region for which the variation in the ^{8}B is larger than 35%.

To obtain the annihilation cross-section for the p-wave annihilation case we numerically solved the Boltzmann equation for the density of a relic particle satisfying the DM abundance as measured today from the CMB. To convert the upper limits on the neutrino flux from the IceCube and SuperKamiokande detectors to upper limits on the WIMP scattering cross-section we used a robust stellar evolution code to model the Sun including DM phenomenology. Assuming that WIMPs distribute isothermally in the Solar core we derived an analytical expression for the annihilation coefficient for the p-wave scenario, which is directly proportional to the Solar central temperature.

Differently from the usual s-wave case (which is commonly adopted adopted in the neutrino analysis present in the literature), the neutrino signal for p-wave annihilating WIMPs will be directionally proportional to the annihilation coefficient, resulting in upper limits on the scattering cross-section at least one order of magnitude above the s-wave case, which reduce the tension with results from other detection experiments.

We also studied the impact of the current uncertainty on Solar models (mainly due to the imposition of different Solar heavy elements mixtures) on our results. We fount out that models with a higher metalicity to Hydrogen ratio have an enhancement of $\sim 20\%$ on the capture rate for SI scattering, while models with lower $(Z/X)_\odot$ capture $\sim 5\%$ more DM for SD scattering. This variations can reflect a maximum of $\sim 4\%$ and $\sim 25\%$ uncertainty on the upper limits for the scattering cross-section for s and p-wave models, respectively.

We would like to acknowledge the authors of the numerical packages used in this work, namely Morel and Lebreton for the stellar evolution code, CESAM; Lopes, Eugénio and Casanellas for including all the DM framework in the code; and finally Blennow, Edsjö and Ohlsson for WimpSim.

The work presented in sec. 3 was orally presented in the *IDPASC Workshop on Space Particles and Earth* at *Universidade de Évora* and in the *GR 100 years in Lisbon* at *Instituto Superior Técnico*. The work developed during section 4 has been submitted for publication in the Astrophysics Journal.

REFERENCES

Aartsen, M.G. et al. 2013, Phys. Rev. Lett., 110, 131302
Ade, P.A.R. et al. 2015, e-Print: arXiv:1502.01589.
Agnese, R. et al. 2013, Phys. Rev. Lett., 111, 251301

Aharmim, B., Ahmed, S.N., Anthony A.E. et al. 2013, Phys. Rev. C, 88(2), 025501
Akerib, D.S. et al. 2014, Phys. Rev. Lett., 112, 091303
Angloher, G., Bauer, M., Bavykina, I., Bento, A., Bucci, C. et al. 2012, Eur. Phys. J., C72, 1971
Aprile, E. et al. 2012, Phys. Rev. Lett., 109, 181301
Asplund, M., Grevesse, N. & Sauval, A.J. 2005, *Astronomical Society of the Pacific Conference Series*, page 25.
Asplund, M., Grevesse, N., Sauval, A.J. & Scott, P. 2009, Annu. Rev. Astron. Astrophys., 47, 481
Bahcall, J.N., Serenelli, A.M. & Basu, S. 2005, ApJ, 621, L85
Bahcall, J.N. & Ulrich, R.K. 1988, Rev. Mod. Phys., 60, 297
Basu, S., Chaplin. W.J., Elsworth, Y., New, R. & Serenelli, A.M. 2009, ApJ, 699, 1403
Bellini, G., Bezinger. J., Bonetti, S. et al. 2010, Phys. Rev. D, 82, 033006
Bellini, G., Bezinger, J., Bick, D., et al. 2011, Phys. Rev. Lett., 107, 141302
Bernabei, R. et al. 2008, Eur. Phys. J., C56, 333
Bertone, G., Hooper, D. & Silk, J. 2005, Phys. Rep., 405, 279
Busoni, G., De Simone, A. & Huang, W. 2013, J. Cosmology Astropart. Phys., 07, 010
Blennow, M., Edsjö, J. & Ohlsson, T. 2008, J. Cosmology Astropart. Phys., 01, 021
Catena, R. & Ullio, P. 2010, J. Cosmology Astropart. Phys., 08, 004
Choi, K. et al. 2015, Phys. Rev. Lett., 114, 141301
Dent, J.B., Dutta, S. & Scherrer, R.J. 2010, Physics Letters B, 687, 275
Drees, M., & Nojiri, M. M. 1992, e-Print: arXiv:hep-ph / 9207234v1.
Faulkner, J. & Gilliland, R.L. 1985, ApJ, 299, 994
Gaisser, T.K., Steigman & G., Tilav, S. 1986, Phys. Rev. D, 34, 2206
Goldberg, H. 1983, Phys. Rev. Lett., 50, 1419
Gould, A. 1987, ApJ, 321, 571
Gould, A. & Raffelt, G. 1990, ApJ, 352, 654
Gondolo, P. & Gelmini, G. 1991, Nucl. Phys. B, 360, 145
Grevesse, N. & Sauval, A.J. 1998, Space Sci. Rev., 85, 161
Griest, K. & Seckel, D. 1987, Nucl. Phys. B, 283, 681
Jungman, G., Kamionkowski, M., & Griest, K. 1996, Phys. Rep., 267, 195
Kim, H.G.& Lee, K.Y. 2007, Phys. Rev. Lett., 75, 115012
Kolb, E.W. & Turner, M.S., *The early Universe*, Addison-Wesley, Redwood City, USA 1989
Lopes, I. & Silk, J. 2010, Science, 330, 462
Lopes, I., Casanellas, J. & Eugénio, D. 2011, Phys. Rev. D, 83, 63521
Morel & P. 1997, A & A Supplement Series, 124, 597
Serenelli, A.M., Basu, S., Ferguson, J.W. & Asplund, M. 2009, ApJ, 705, L123
Serenelli, A. 2010, Asrophys. Space Sci., 328, 13
Shelton, J., Shapiro, S., & Fields, B. 2015, Phys. Rev. Lett., 115, 23
Sheldon, C., Dutta, B., & Komatsu, E. 2010, Phys. Rev. D, 82, 9
Silk, J., Olive, K., Srednicki & M. 1985, Phys. Rev. Lett., 55, 257
Sjöstrand, T., Mrenna, S. & Skands, P. 2006, J. High Energy Phys. , 05, 026
Spergel, D.N. & Press, W.H. 1985, ApJ, 294, 663
Steigman, G., Sarazin,C.L., Quintana, H. & Faulkner, J. 1978, AJ, 83, 1050
Turck-Chieze, S. & Lopes, I. 1993, ApJ, 408, 347
Yoon, S.C., Iocco, F. & Akyiama, S. 2008, ApJ, 688, L1
Wilkstrom, G. & Edsjo, J. 2009, J. Cosmology Astropart. Phys., 04, 009